INTRODUCING NEW VITREOUS CUTTER BLADE SHAPES

A Fluid Dynamics Study

TOMMASO ROSSI, MD,* GIORGIO QUERZOLI, PHD,† GIAMPIERO ANGELINI, DENG,‡
CARLO MALVASI, DENG,‡ MARIO IOSSA, MD,* LUCA PLACENTINO, MD,* GUIDO RIPANDELLI, MD§

Purpose: To assess the efficacy of novel vitreous cutter blades compared with the regular guillotine by means of particle image velocimetry. Tested blades included a regular blade (RB) and newer designs where a circular (hole blade [HB]) or a slit aperture (slit blade [SB]) had been opened proximal to the cutting edge.

Methods: Twenty-three–gauge probes were immersed in BSS or egg albumen, and high-speed video (1,000 frames per second) was recorded. Duty cycle, flow rate, and acceleration generated by Venturi and peristaltic pumps were measured under cutter settings simulating "low-speed" vitrectomy (1600 cuts per minute, 200 mmHg vacuum) and "high speed" vitrectomy (3000 cuts per minute, 300 mmHg vacuum).

Results: The SB and HB had a significantly more favorable duty cycle than that of the RB ($P < 0.01$) and higher BSS flow rate regardless of the aspiration. The SB flow rate in albumen was significantly higher than that of the HB and RB only over 1,000 cuts per minute using a peristaltic pump and at any cut rate with Venturi pump ($P < 0.001$). The SB also yielded the lowest fluid acceleration than both the HB and SB ($P < 0.001$ in all cases).

Conclusion: The HB and SB proved to be significantly more efficient than the RB, with better duty cycle and higher flow rate. The SB generated significantly less fluid acceleration than any other tested blade, regardless of the fluid viscosity and pump technology. The SB design is significantly more efficient and possibly safer than both HB and RB.

RETINA 0:1–9, 2014

Vitreous cutters have greatly improved since Machemer's VISC, mostly because of the miniaturization of probes and the use of electronics for duty cycle, aspiration, and infusion control. Although the gauge greatly reduced with time and cutter port moved slightly toward the instrument tip, the port and blade design remained unchanged for the past 40 years.

Fluid dynamics of vitrectomy probes has been characterized by means of particle image velocimetry.[1] Duty cycle, with the flow rate and acceleration identified as clinically significant measures of vitreous removal efficiency and retinal traction.

The purpose of this article is to introduce newly designed vitreous cutter blades and compare their fluidics with the regular guillotine aiming to test the hypothesis that modified blades can increase the flow rate while reducing fluid acceleration, thus improving both efficacy and safety.

Materials and Methods

Blade Shapes

We compared three different blade shapes:

- A regular guillotine blade (RB) (Figure 1A)
- A hole blade (HB) (Figure 1B) in which a 0.1-mm diameter hole had been drilled in a position that corresponds to the center of the port when the blade closes

From the *Eye Hospital of Rome, University of Cagliari, Cagliari, Italy, FAculty of Engineering, DICAT Department, Bietti Foundation IRCCS, Rome, Italy, Optikon 2000 Inc, Rome, Italy; †University of Cagliari, DICAAR; ‡Optikon 2000 Inc; and §Fondazione G.B. Bietti, IRCCS.

G. Angelini and C. Malvasi are employees of Optikon 2000 Inc. The other authors have no financial/conflicting interests to disclose.

Reprint requests: Tommaso Rossi, MD, Via Tina Modotti 93, Rome 00142, Italy; e-mail: tommaso.rossi@usa.net

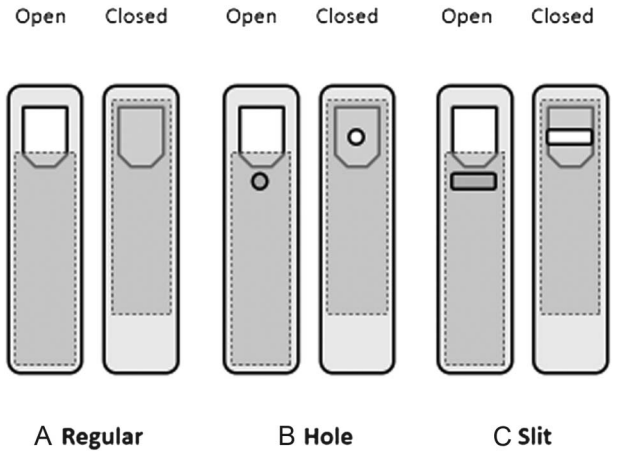

Fig. 1. Schematic drawing of blade shapes. **A.** The RB, guillotine shaped, obstructs completely the port when closed. **B**. The HB has a 0.1-mm-wide hole in the middle of the port area when closed. **C.** The SB has a 0.1-mm-wide rectangular opening in the middle of the port and encompassing the entire port width.

- A slit blade (SB) (Figure 1C) in which a 0.1-mm-wide slit with cutting edges was cut across the inner cylinder, projecting in the center of the port when the blade closes.

Experimental Setting

Twenty-three–gauge probes mounting the above blades connected to R-Evolution vitrectomy machine (Optikon 2000 Inc, Rome, Italy) equipped with double Venturi/peristaltic pump have been tested under various combinations of cut rate and aspiration settings (Table 1) to simulate 2 typical surgical scenarios: low speed "core" vitrectomy and relatively high-speed vitreous base "shaving." Cutters were secured vertically with the distal 20-mm probe tract immersed in a transparent Plexiglas box ($3 \times 5 \times 3$ cm parallelepiped) filled with BSS (Alcon, Forth Worth, TX), or egg albumen,[2] to simulate both aqueous and vitreous-like fluidics.[3]

Table 1. Vitreous Cutter Settings: Venturi (V) and Peristaltic (P) Pumps Were Used in All Tests With Suction and Cut Rate Set at Typical Low-Speed "Core Vitrectomy" and High-Speed "Shave Vitrectomy" Combinations

Modality	Cut Rate, Cuts Per Minute	Aspiration, mmHg	Pump: Venturi, Peristaltic
Low speed ("Core")	1600	200	V and P
High speed ("Shave")	3000	300	V and P

The peristaltic pump was set at 15 mL/minute flow rate in all cases.

To allow fluid motion detection and particle image velocimetry measures, BSS was seeded with triamcinolone crystals (Kenakort, Brystol-Myers Squibb, New York, NY) passed through a 40-μm filter and egg albumen with air microbubbles.

A 2-mm-wide slit of light was shed directly onto the cutter port 90° away from the light-source and the camera focused on the plane of the vitreous cutter port, which was oriented directly toward the light (i.e., at 90° from the camera view), as described elsewhere.[1]

High-Speed Imaging

Fluid motion around the cutter port was recorded for 2 consecutive seconds using MotionPro high-speed camera (Integrated Design Tools Inc, Tallahassee, FL) and stored as uncompressed audio–video interleaved format (.avi) movie (the frame rate was 1000 frames per second and resolution 1024×1280 pixel for all measures expect duty cycle calculations, when the camera run at 3,000 fps). Five seconds was allowed between the vitreous cutter onset and video recording, to skip the transitional phase.

Particle Image Velocimetry

Particle image velocimetry measures fluid velocity from high-speed movies by recognizing the motion of tracers dispersed in fluid (i.e., triamcinolone crystals or microbubbles). Corresponding windows on the successive images are compared under the assumption that tracers translate in subsequent frames conserving their brightness. The displacement minimizing the dissimilarity between the corresponding windows is assumed to be representative of fluid motion in that region. For image analysis, we used robust imaging velocimetry, as applied to ophthalmology elsewhere.[1,4] Compared with the classic particle image velocimetry algorithm, robust imaging velocimetry uses a measure of dissimilarity, which is statistically robust to outliers and therefore less affected by noise, artifacts, or by velocity gradients within the interrogation window.[1]

Main Outcome Measures

Duty cycle, defined as the percentage of open port surface as a function of time, was measured on frame-by-frame video analysis. The volumetric flow rate has been calculated from particle velocity within the aspiration tubing, whose internal diameter is known (since flow = velocity × internal tubing aperture surface).

To derive fluid acceleration, kinetic energy of a given perturbed fluid volume around the cutter port

was also calculated. Kinetic energy has been defined as the spatial average at a given instant of the local kinetic energy per unit mass (which is $1/2V^2$, where V is the velocity). The investigation area was 20.8×26 mm wide. Acceleration was then calculated as twice the time derivative of the square root of kinetic energy.

Statistical Analysis

Testing the significance of curve difference poses peculiar problems and several techniques have been proposed.[5] The flow rate data were analyzed by means of *t*-test when peristaltic and Venturi pump results of the same blade and setting were considered while single factor analysis of variance (ANOVA) with Bonferroni post hoc tests has been implied when acceleration of the 3 blades was compared.

Significance (P) has been set at the 0.05 level in all cases except when the Bonferroni procedure was involved (such as when comparing the 3 blades), in which cases, $\alpha = 0.05$ was divided for the overall number of tests ($\alpha = 0.05/3 = 0.0167$).

Results

Duty Cycle and Flow Rate

Duty cycle comparison (Figure 2) shows an advantage for the SB followed by the HB and the RB (ANOVA, $P < 0.01$ in all cases) because of the residual port opening surface represented by the slit and hole, respectively, when the port is closed.

The BSS flow rate at 200 mmHg suction (Figure 3A) shows an advantage for both SB and HB over RB at cut rates over 1600 cuts per minute (cpm) (ANOVA; $P < 0.001$ SB vs. RB and HB vs. RB; SB vs. HB not significant). At 300 mmHg aspiration (Figure 3B), SB and HB yield a higher flow rate compared with RB, regardless of the cut rate (ANOVA, $P < 0.001$ in all cases; SB vs. HB not significant).

The egg albumen flow rate data (Figure 4) show an advantage for SB and HB over RB whenever a peristaltic pump is used over 1,000 cpm (Figure 4, A and B). When a Venturi pump is used, SB yields higher flow rates regardless of the cut rate (ANOVA, $P < 0.01$), whereas HB and RB perform similarly.

BSS Fluidics

The Balanced Salt Solution (BSS, Alcon, Forth Worth, TX) acceleration (Figure 5) is greatly impacted by blade design: RB accelerates BSS almost 10 times more than HB and SB, with a significant reduction in the amplitude with a trend of RB >> HB > SB ($P < 0.001$ for all pairs; see Figure 6 at higher scale for HB Vs SB comparison). The HB BSS acceleration peaks also show a significant association with pump technology: the peristaltic pump determines higher acceleration peaks (*t*-test, $P < 0.01$ both at 1600 cpm, 200 mmHg vacuum: [Figure 6 A vs. C] and at 3000 cpm, 300 mmHg vacuum [Figure 6 B vs. D]). The SB-induced BSS acceleration does not change significantly with different pumps (*t*-test, P not significant).

Albumen Fluidics

The HB determines the highest albumen acceleration peaks (Figure 7), regardless of the cut rate and pump type ($P < 0.0001$ in all cases), especially at 1600 cpm when a peristaltic pump is used (Figure 7A). The RB

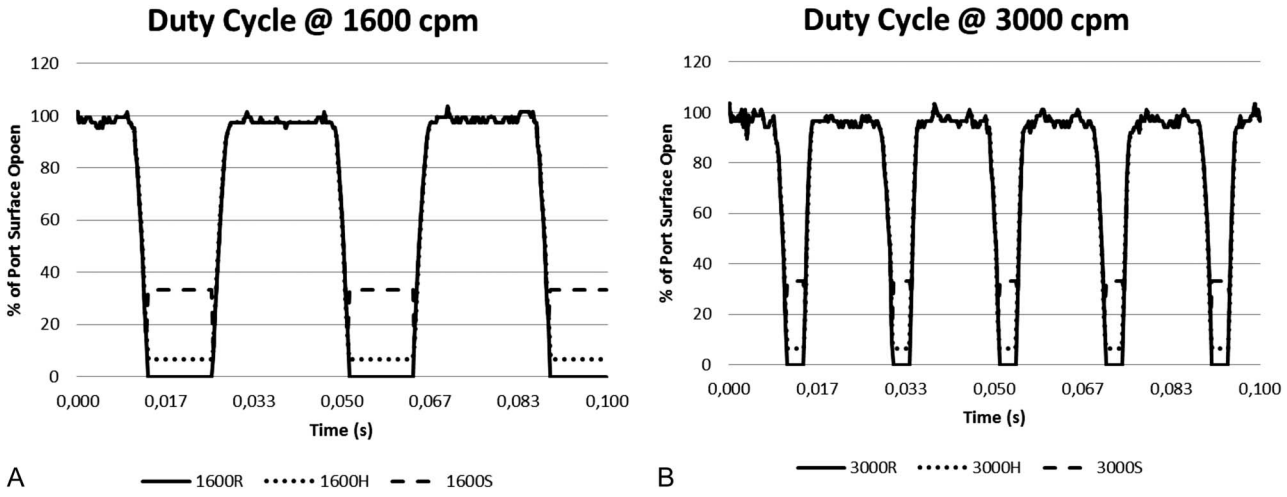

Fig. 2. Duty cycle of RB, HB and SB blades at 1600 (**A**) and 3000 (**B**) cpm. Note that the presence of a hole (dotted line) or slit (dashed line) determines a residual opening when the blade closes and determines an increase in the overall duty cycle defined as the percentage of pervious surface per entire cutting cycle.

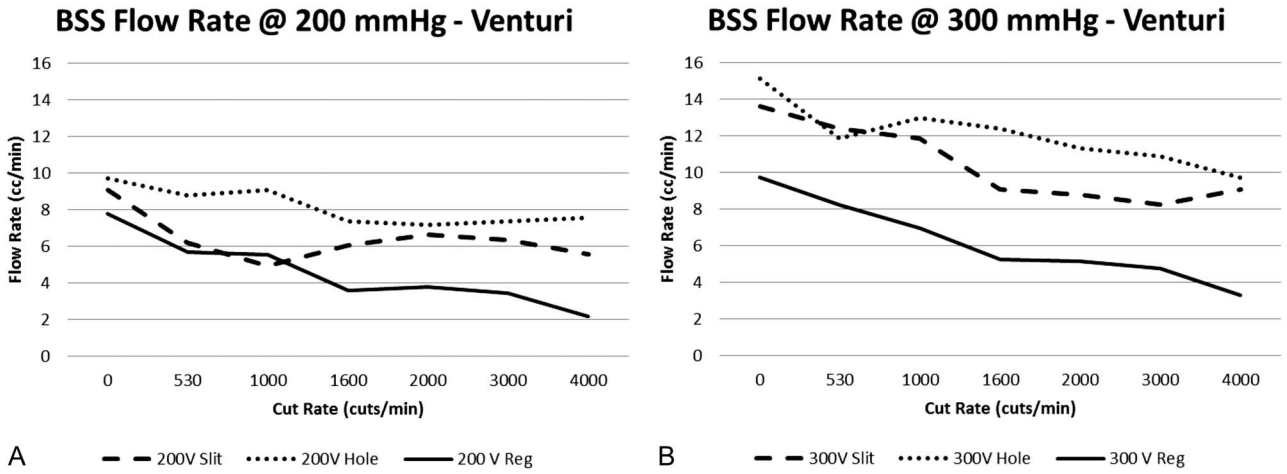

Fig. 3. BSS volumetric flow rate at 200 mmHg (**A**) and 300 mmHg aspiration (**B**). Note that the RB shows the lowest flow rate at all cut rates and that HB and SB show a higher flow than the RB. The advantage of modified blades (SB and HB) increases with the cut rate because of a less favorable duty cycle as the cut rate increases.

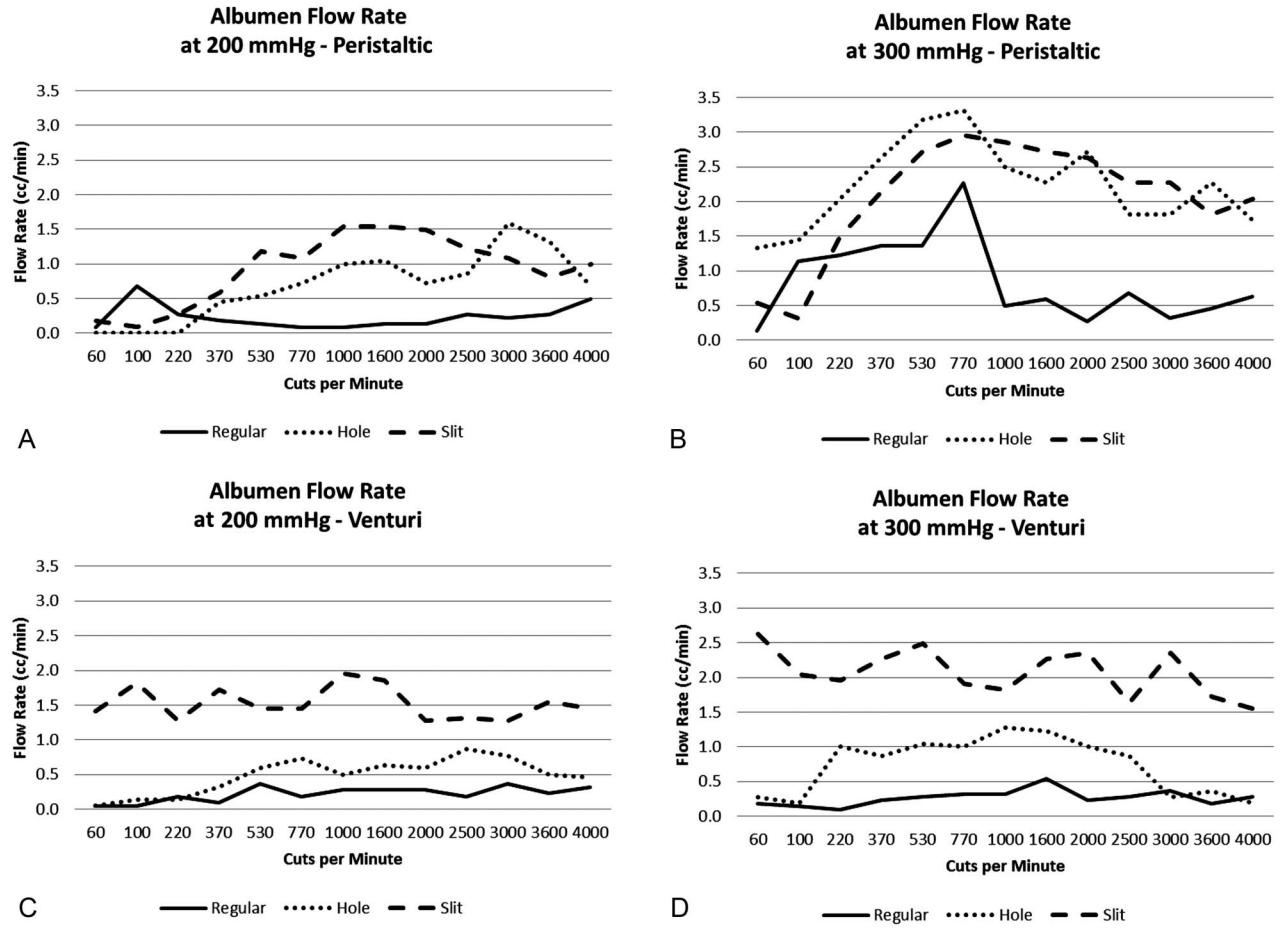

Fig. 4. Albumen volumetric flow rate at 200 mmHg aspiration (**A** and **C**) and 300 mmHg aspiration (**B** and **D**) for peristaltic (**A** and **B**) and Venturi pump (**C** and **D**). Note that in all cases, the RB allows the lowest flow rate and that the peristaltic pump shows lower flow rates at low cut rates compared with the Venturi. The SB always shows the highest flow, similar to the HB only when a peristaltic pump is used and significantly higher than both HB and RB, when a Venturi pump is engaged.

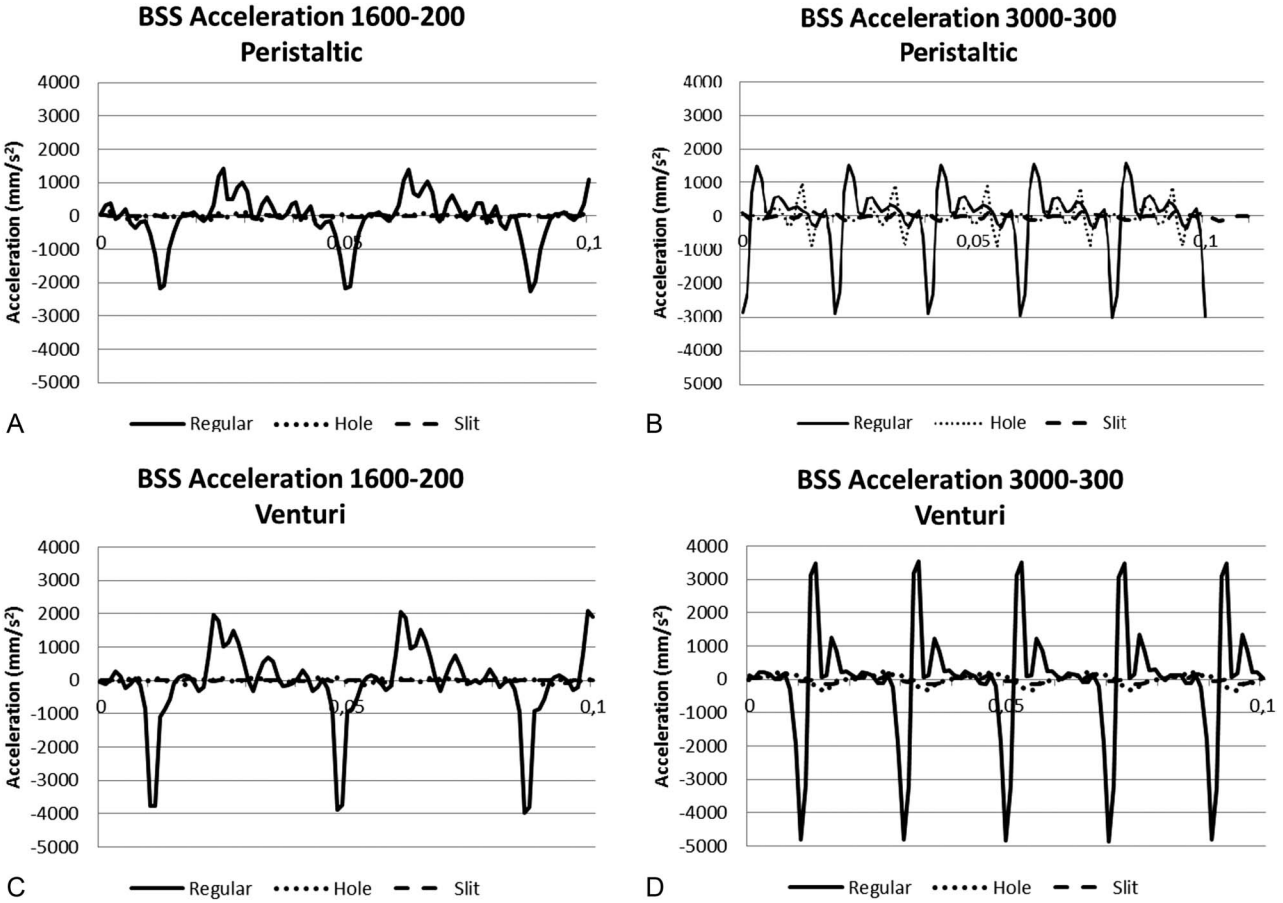

Fig. 5. The BSS acceleration. The x-axis represents time in seconds and spans 0.1 seconds. The RB produces the highest acceleration peaks in all cases (dashed line). See Figure 6 for a more detailed HB versus SB comparison. Peristaltic pump generates higher acceleration peaks than the Venturi at the corresponding cut rate and suction settings (**A** vs. **C** and **B** vs. **D**). Note that at lower cut rate, the RB creates higher acceleration and that the peristaltic pump tends to generate higher peaks.

also generates significantly higher acceleration than the SB. The pump type largely influences the acceleration: at 200 mmHg of suction, the peristaltic pump always determined significantly higher acceleration when comparing the same blades (*t*-test, $P > 0.001$ in all cases). At 300 mmHg suction, the peristaltic pump yielded lower acceleration with HB and RB (*t*-test, $P < 0.001$ in both cases), whereas no significant difference among pumps could be calculated for the SB (*t*-test, *P* not significant).

Discussion

This article compares the fluidics of regular vitreous cutter blades (RB) with novel shapes engineered to improve flow and reduce fluid acceleration.[6] We replicated the hole blade reported by Rizzo et al[7] (Figure 1B, HB) and proposed a novel slit aperture blade (Figure 1C, SB) that offers the advantage of doubling the cut rate, thus retaining a more favorable duty cycle than the HB and RB.

Duty cycle is in fact one of the key factors influencing flow and traction, especially at higher cut rates.[8–10] The SB has the most favorable duty cycle, followed by HB and RB (Figure 2) because of the wider opening and the improvement in the BSS flow (Figure 3) rises with the cut rate, given the proportionally higher criticality of closure phase at higher speed.

Fibril-structured albumen flow behaves differently from BSS (Figure 4): the SB allows the highest flow in all testing conditions, whereas the HB performs comparably with SB only when using a peristaltic pump (Figure 4, A and B). One possible explanation relates to pump functioning mechanism and aperture size: a peristaltic pump builds up negative pressure until a given volume of fluid is removed, increasing pressure also within the cutter shaft, when the blade obstructs the port. Therefore, if a hole or slit is opened through the closed port, suction continues to grasp and pull the fibrils inside the port. As an adjunctive

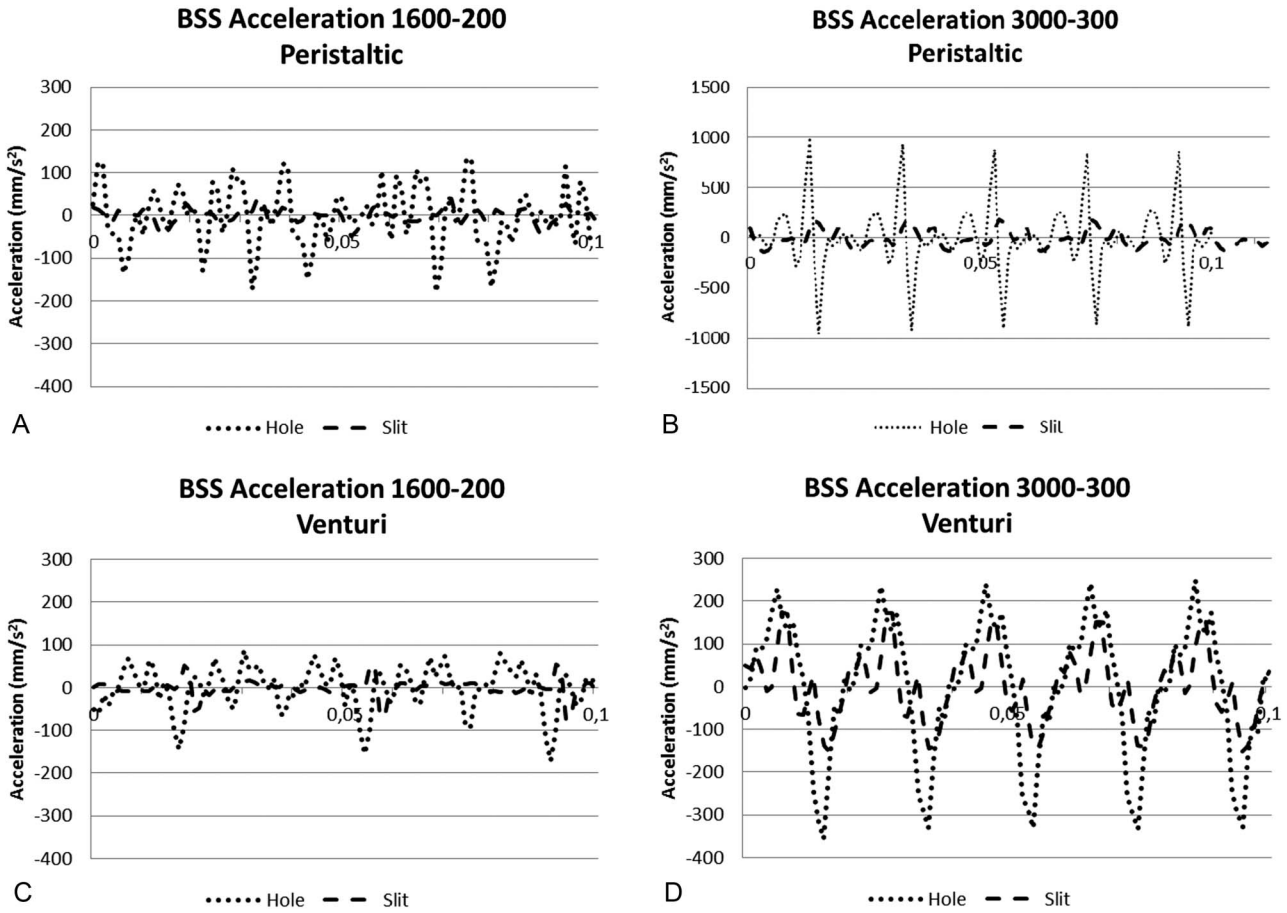

Fig. 6. The BSS acceleration for HB and SB only. The x-axis represents time in seconds and spans 0.1 seconds. The same data as in Figure 4 are presented, excluding RB data, to show the difference between HB and SB on a larger scale. Note that the y-axis scale in **B** is greater. The HB determines a higher fluid acceleration than SB in all cases and peristaltic pumps tend to generate higher acceleration compared with Venturi pumps under similar aspiration settings. $p < 0.05$.

mechanism, the slit, and to a lesser extent the hole, works as additional blades, severing engaged collagen especially at higher cut rates when the shear rate is higher.[10] It should be noted that in albumen, aspiration alone does not generate flow because the high and fibril structure clog the inner lumen. Only after cutting is engaged, the long fibril chains are severed into little chunks; within certain limits, the smaller the chunks, the better. (Figure 4, at lower cut rates, the RB and HB flow is actually the lowest for this very reason). It is our opinion that the SB acts as a much more efficient adjunctive blade than the HB both because of the wider aperture size and the cutting-edge design accuracy.

When using a Venturi pump, SB generates the highest flow regardless of the cut rate, whereas HB and RB (Figure 4, C and D) do not differ significantly, probably because the hole surface is too small to generate an efficient flow at the lower pressures gradients generated by a Venturi pump, even at high shear rate.

Fluid acceleration was analyzed as a way to predict retinal traction, based on the assumption that in the living eye, the vitreous is firmly attached to the retina and force equals mass times acceleration (F = ma). Under such circumstances, a blade capable of inducing the least fluid acceleration is to be considered safer.

The cyclic rise and fall of acceleration beating exactly at cut rate pace (Figures 5 and 7) testifies that the blade motion generates intermittent flow through periodic port obstruction that conditions flow rate (Figures 3 and 4) and is responsible for fluid velocity changes (i.e., acceleration), aspiration efficiency, and ultimately, traction. Improving vitreous cutter performance therefore implies increasing flow while reducing acceleration in proximity of the port, ideally achieving constant velocity. Fluid acceleration, in fact, generates pressure variations that engages vitreous, resulting in retinal traction. Teixeira et al[11,12] measured the force exerted on the retina as a function of blade duty cycle, proving

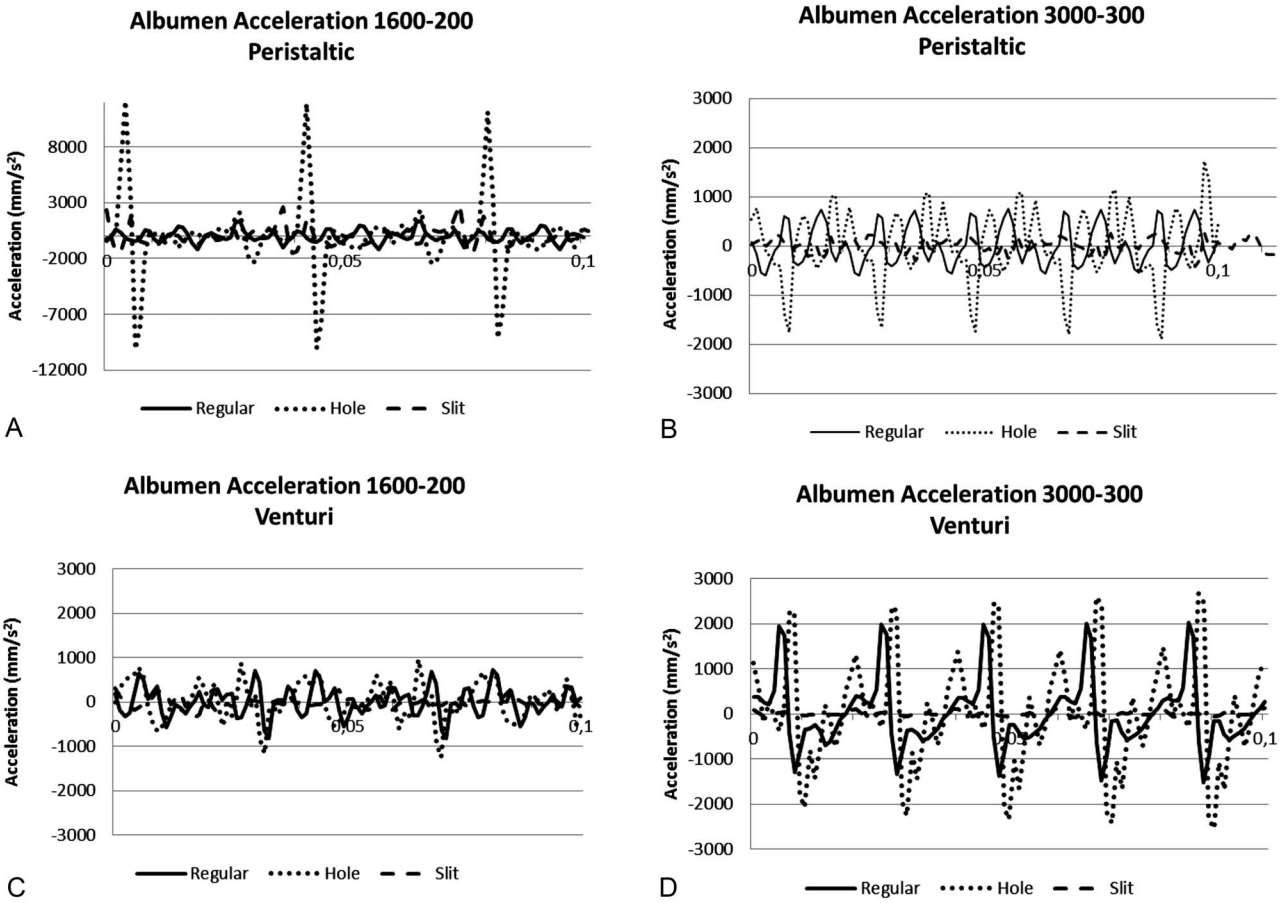

Fig. 7. Albumen acceleration. The x-axis reports time in seconds and spans 0.1 seconds. Note that **A** has a much greater y-axis scale. The HB (dotted line) shows the highest acceleration regardless of the pump and cut rate/suction combination. The SB retains the lowest acceleration in all tested conditions. $p < 0.05$.

the cause–effect relation between blade-motion and retinal traction.

The RB yield the highest BSS acceleration (Figure 5) followed by the HB and SB (Figure 6). Within the Newtonian low-viscosity BSS, the alternating complete port obstruction and sudden suction due to port opening is probably the reason why the RB causes the highest acceleration (Figure 5D), followed by the HB and SB that allow an increasingly higher residual flow when the port is only partially closed by the blade, thus reducing velocity changes.

The HB accelerates albumen the most, especially when the peristaltic pump is used at lower cut rates (Figure 7A), followed by the RB and SB (Figure 7). A possible explanation is as follows: regardless of the blade design, all ports engage the long elastic collagen fibrils when open but only the HB and SB keep engaging albumen when the port closes. The HB, however, is less efficient than the SB in severing engaged fibrils though the "secondary aperture" (the hole), because of smaller dimension of residual aperture and a less favorable cutting edge. As a result, HB pulls and "shakes" collagen whereas SB cuts it, resulting in a much lower acceleration, as shown in Figure 7.

Throughout all tested settings, the SB consistently generated the least acceleration, showing minimal dependence on blade motion and approaching the ideal condition of a "constant-flow vitrectomy."

Lima et al[13] designed various dual-port vitreous cutter probes concluding that although some of them improved flow rate, there was no clinical benefit and some were disadvantageous while performing high speed vitrectomy. Although they did not perform any fluidics analysis, it is conceivable that a wider or double port simply allows an increased flow rate because of the increased overall port size, leaving the mechanism of alternated suction and cutting unaltered, which is responsible for an even greater acceleration and deceleration. In addition, the larger outer port surface increases the risk of inadvertent retinal engagement.

Acceleration versus flow rate scattergrams in BSS (Figure 8) and albumen (Figure 9) add one more useful piece of information: different blades tend to cluster on different sides of the line bisecting the chart.

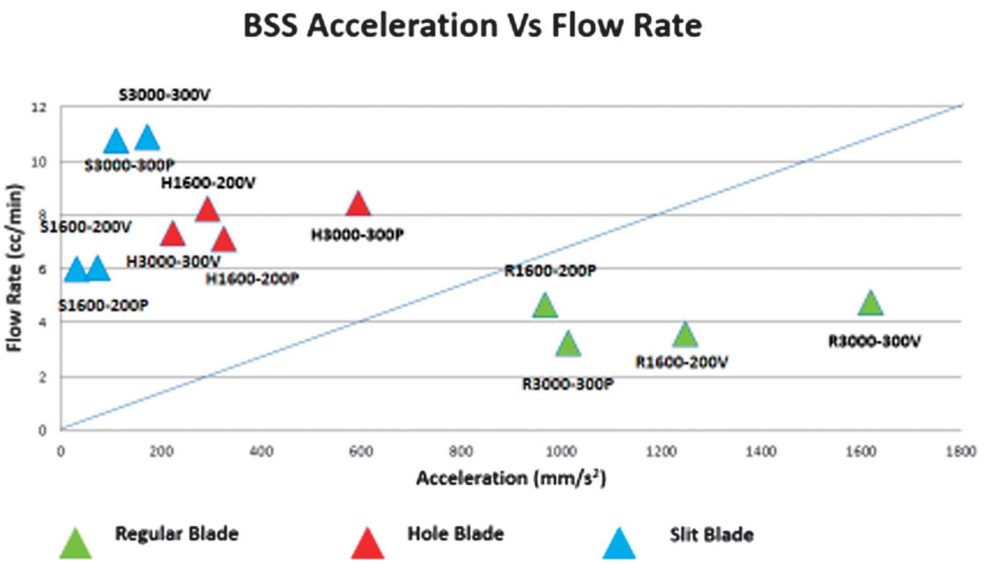

Fig. 8. The BSS average acceleration versus flow rate: XY scattergram. Note that different settings of the same blade tend to cluster and project on different sides of the chart bisector line. Overall, all setting combinations of the SB (blue triangles) offer a higher flow combined with lower acceleration, as opposed to the RB cluster (green triangles) that tends to project in the lower right quadrant. The HB cluster shows a tendency toward lower flow and higher acceleration than SB.

COLOR

On the base of flow and fluid acceleration, the scattergram can be divided into 4 quadrants (Figure 10) identifying cutter behavior. We propose the use of such scattergram as a benchmark for cutter safety and efficiency: a low flow rate and acceleration denote inefficient blades (Figure 10, lower left), whereas high flow and acceleration mark dangerous setting/blades combinations (Figure 10, upper right). Low flow and high acceleration speak for inefficient and dangerous settings/blades (Figure 10, lower right) and high flow and low acceleration (Figure 10, upper left) probably represent the most desirable setting/blades combination.

It is also noteworthy that the same blade/setting combination falls into different areas of the scattergram when tested in different media: in BSS (Figure 8) the HB allows high flow and low acceleration, falling into the upper left quadrant, whereas the RB stands on the lower right. When albumen measures are considered (Figure 9), the HB results tend to project below the bisector line and lower right quadrant, whereas the RB data cluster within the least efficient region of the chart. The SB results, instead, steadily remain in the upper left quadrant, testifying the higher efficiency of such design.

In summary, our data strongly suggest that shaping blades can offer significant advantages from the fluidics standpoint. In particular, the SB increases the flow while minimizing acceleration and doubling cut

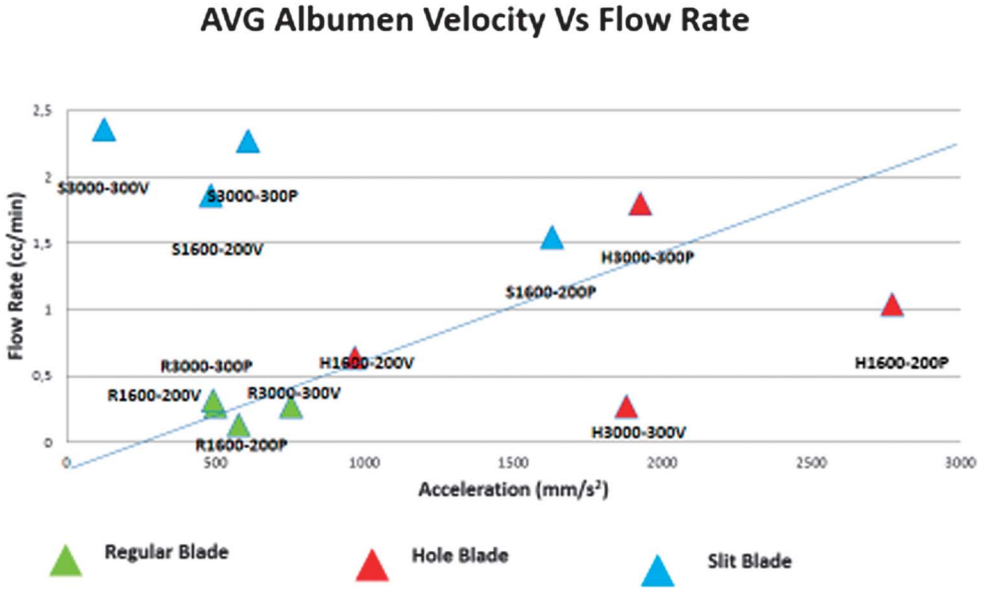

Fig. 9. Albumen average acceleration versus flow rate; XY scattergram. Note that different settings of the same blade tend to cluster and project on different sides of the chart bisector line. The SB (blue triangles) tend to cluster in the upper left quadrant, evidencing a higher flow and lower acceleration when compared with the RB cluster (green triangles) that is localized in the lower left quadrant, evidence of scarce efficiency. The HB (red triangles), although a little more dispersed, localize inferiorly to the bisector line and toward the rightmost part of the chart, because of a dangerously high acceleration and lower flow than the SB.

COLOR

COLOR

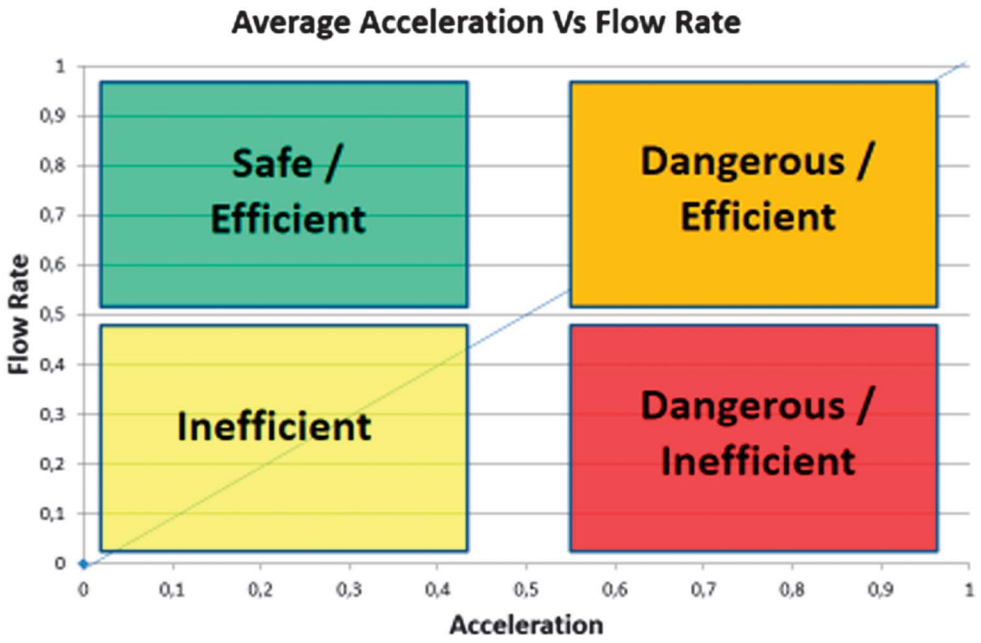

Fig. 10. Acceleration versus flow rate; XY schematic scattergram showing how the entire chart can be ideally divided into 4 regions characterizing different operative features. Vitreous cutter setting/blades can be intuitively labeled as "safe," "unsafe," "inefficient," or "dangerous," depending on the region of the scattergram where they fall.

rate, thus clearly outperforming both the HB and the RB. We believe this can be used as a proof of principle that different blades and possibly port shapes can provide better fluidics control and a safer and more efficient vitrectomy; we also propose a simple way to categorize cutter behavior based on acceleration and flow.

Limitations of this study include the use of egg albumen to simulate vitreous and the relatively low number of vitrectomy setting combinations studied. However, albumen is frequently used[2] as a low-cost, readily available, and more importantly, more stable and consistently fibril-structured medium than cadaver or porcine vitreous that quickly liquefy.

Particle image velocimetry analysis could have been extended to a higher number of cut rate/aspiration combinations although those "paradigmatic" settings we tested clearly generated significant results. Different surgeons use different cut rate and aspiration combinations and therefore a larger parametric study on multiple variables associated to vitreous cutter machine adjustment remains desirable.

Further tests on porcine vitreous and human cadaver eyes will help elucidating whether the idea of multiple and fissured blades can replace the traditional guillotine and establishing the most efficient combination of slit and port dimension.

Key words: particle image velocimetry, vitreous cutter fluidics, vitreous traction, human vitreous motion, pars plana vitrectomy, vitreous acceleration.

References

1. Rossi T, Querzoli G, Angelini G, et al. Fluid dynamics of vitrectomy probes. Retina 2014;34:558–567.
2. Wals KT, Friberg TR. Vitreous substitute removal rates with the accurus and millennium vitrectomy systems. Ophthalmic Surg Lasers Imaging 2008;39:174–176.
3. Pitcher JD III, McCannel CA. Characterization of the fluidic properties of a syringe-based portable vitrectomy device. Retina 2011;31:1759–1764.
4. Falchi M, Querzoli G, Romano GP. Robust evaluation of the dissimilarity between interrogation windows in image velocimetry. Exp Fluids 2006;41:279–293.
5. Fan J, Sheng-Kuei L. Test of significance when data are curves. J Am Stat Ass 1998;443:1007–1021.
6. Thompson JT. Advantages and limitations of small gauge vitrectomy. Surv Ophthalmol 2011;2:162–172.
7. Rizzo S. Performance of a modified vitrectomy probe in small-gauge vitrectomy. Retina Today 2011;9:40–42.
8. Fang SY, DeBoer CM, Humayun MS. Performance analysis of new-generation vitreous cutters. Graefes Arch Clin Exp Ophthalmol 2008;246:61–67.
9. Steel DH, Charles S. Vitrectomy fluidics. Ophthalmologica 2011;226:27–35.
10. Magalhaes O Jr, Chong L, DeBoer C, et al. Vitreous dynamics: vitreous flow analysis in 20-, 23-, and 25-gauge cutters. Retina 2008;28:236–241.
11. Teixeira A, Chong L, Matsuoka N, et al. An experimental protocol of the model to quantify traction applied to the retina by vitreous cutters. Invest Ophthalmol Vis Sci 2010;51:4181–4186.
12. Teixeira A, Chong LP, Matsuoka N, et al. Vitreoretinal traction created by conventional cutters during vitrectomy. Ophthalmology 2010;117:1387–1392.
13. Lima LH, DeBoer C, McCormick M, et al. A new dual port cutter system for vitrectomy surgery. Retina 2010;30:1515–1519.